



## Possible Beneficial Molecular Effects of Nano-Chitosan Against Manganese Genotoxicity in the Nile Tilapia (*Oreochromis niloticus*) Using SCoT Molecular Markers

Anas A. Heiba<sup>1\*</sup>, Medhat H. Hashem<sup>1</sup>, Midhat A. El-Kasheif<sup>2</sup>, Ebrahim A., Sabra<sup>1</sup>, Aya Y. Gad<sup>1</sup>

<sup>1</sup>Animal Biotechnology Department, Genetic Engineering and Biotechnology Research Institute (GEBRI),  
University of Sadat City (USC), Sadat City, Egypt

<sup>2</sup>National Institute of Oceanography and Fisheries, Cairo, Egypt

\*Corresponding Author: anas-heaba@hotmail.com

### ARTICLE INFO

#### Article History:

Received: April 15, 2025

Accepted: July 19, 2025

Online: July 27, 2025

#### Keywords:

Chitosan nanoparticles,  
Manganese genotoxicity,  
*Oreochromis niloticus*,  
SCoT markers

### ABSTRACT

The escalating contamination of aquatic ecosystems with heavy metals, such as manganese (Mn), poses a significant threat to aquatic life, particularly fish. Mn toxicity can induce oxidative stress and DNA damage, thereby compromising fish health and survival. The present study aimed to evaluate the potential protective effects of chitosan nanoparticles (CS NPs) against Mn-induced genotoxicity in the Nile tilapia (*Oreochromis niloticus*) using Start Codon Targeted (SCoT) polymorphism analysis. The experimental design included two Mn exposure concentrations (45 and 27mg/ L) combined with two levels of CS NPs supplementation (1.0 and 0.5g/ kg of feed). Water quality parameters were carefully monitored throughout the experiment. At the end of the exposure period, DNA was extracted from muscle tissue, and SCoT-PCR analysis was performed using ten different primers. The SCoT analysis revealed that Mn exposure, particularly at 45mg/ L, significantly increased DNA damage. Supplementation with CS NPs, especially at 0.5g/ kg of feed combined with 27mg/ L Mn exposure, demonstrated a notable protective effect by restoring the genetic profile to a state like that of the control group, thereby mitigating Mn-induced genotoxicity. Interestingly, treatment with CS NPs alone (0.5g/ kg of feed) also resulted in the presence or absence of bands with some primers, suggesting a potential genotoxic effect of CS NPs themselves. These findings indicate that CS NPs may have a protective role against Mn-induced genotoxicity in the Nile tilapia at lower Mn concentrations. However, the observed DNA changes following CS NPs treatment alone underscore the need for caution. Further research is required to elucidate the underlying molecular mechanisms of CS NPs' protective effects—such as their ability to reduce oxidative stress or enhance DNA repair—and to determine the optimal and safe concentrations for mitigating heavy metal toxicity in aquatic organisms.

### INTRODUCTION

Aquaculture plays a pivotal role in ensuring global food security, and continuous advancements are imperative to sustainably meet the escalating global demand for aquatic food products (Boyd *et al.*, 2020). However, the intensification of aquaculture operations is increasingly challenged by environmental pollution, particularly heavy metals, which pose a significant threat to both farmed fish and the integrity of aquatic ecosystems (Bayomy *et al.*, 2015; Bukola *et al.*, 2015). Manganese (Mn), a prevalent heavy metal pollutant, enters aquatic environments through diverse anthropogenic sources, including industrial and

agricultural activities, leading to widespread contamination (**Authman *et al.*, 2013; Monier *et al.*, 2023**). While Mn is a micronutrient essential for various biological processes (**Shiau & Hsieh, 2001; Lall, 2002**), it becomes a hazardous pollutant at elevated concentrations.

Elevated Mn levels in aquatic habitats exert significant toxicological pressure on aquatic organisms. Fish exposed to Mn can suffer a range of adverse effects, including neurological damage, behavioral abnormalities (**Sharma *et al.*, 2019**). These impacts also include the compromised physiological functions (**Lall, 2002**). Understanding the genetic consequences of Mn exposure is crucial for assessing long-term impacts on fish populations and developing effective mitigation strategies (**Liu & Cordes, 2004**). Genetic alterations induced by heavy metals can impair the adaptive capacity of fish, potentially leading to reduced fitness and increased vulnerability to environmental changes (**Carvalho & Hauser, 1998**). For example, **Heiba *et al.* (2021)** documented significant genetic variations in the Nile tilapia (*Oreochromis niloticus*) exposed to pollutants in the River Nile, highlighting the direct impact of environmental contaminants on fish genetic integrity. Therefore, investigating the genotoxic effects of Mn is paramount for safeguarding the genetic integrity of aquaculture species.

In recent years, chitosan nanoparticles (CS NPs) have emerged as a promising tool in aquaculture, offering a multifaceted approach to enhance fish health and environmental sustainability (**Wang & Li, 2011**). CS NPs, derived from the naturally abundant polysaccharide chitosan, possess unique characteristics—biodegradability, biocompatibility, and a large surface area—making them ideal for various applications in aquaculture and environmental management (**Abd El-Naby *et al.*, 2019**). Notably, CS NPs have demonstrated potential in mitigating heavy metal toxicity through mechanisms such as adsorption and chelation, effectively reducing heavy metals' bioavailability and protecting aquatic organisms from harmful effects (**El-Shafei *et al.*, 2021**). Furthermore, CS NPs have been explored for their immunostimulatory (**Hussein *et al.*, 2021**) and growth-promoting properties in fish, suggesting a holistic approach to enhancing resilience and productivity in aquaculture systems. Additionally, they are being investigated for mitigating heavy metal genotoxicity through multiple mechanisms, including the adsorption of metal ions and the inhibition of oxidative stress.

To detect and characterize genetic changes induced by environmental stressors like Mn, molecular markers offer unprecedented precision and sensitivity. The start codon targeted (SCoT) polymorphism, a PCR-based marker system developed by **Collard and Mackill (2009)**, has become a valuable tool for gene-targeted marker development and genetic diversity analysis (**Abu Almaaty *et al.*, 2020**). SCoT markers are designed to amplify conserved regions flanking the ATG start codon—a highly conserved site in genes—providing direct insights into gene-coding regions of the genome. These regions are sensitive to genetic alterations caused by environmental stressors, making SCoT markers suitable for assessing genotoxic effects (**Collard & Mackill, 2009; Xiong *et al.*, 2011**). The SCoT technique is advantageous for its technical simplicity, high reproducibility, and cost-effectiveness, enabling efficient screening of genetic polymorphisms (**Kumar & Gurusubramanian, 2011; Amirmoradi *et al.*, 2012; Bhattacharyya *et al.*, 2013**). SCoT markers have been widely applied in genetic studies, including diversity assessments, cultivar

identification, and evolutionary biology—primarily in plants (Poczai *et al.*, 2013; Cabo *et al.*, 2014; Chen & Li, 2014; Que *et al.*, 2014). However, their application is expanding into animal genetics, including fish, particularly for population studies and assessing genotoxic impacts of environmental pollutants (Abu Almaaty *et al.*, 2020). The gene-targeted nature of SCoT markers makes them especially useful for investigating functional genetic variations and adaptive responses to environmental challenges. Furthermore, Hashem *et al.* (2020a) utilized the inter simple sequence repeat (ISSR)-PCR to assess genetic variation in the Nile tilapia exposed to pollution in the El-Rahawy Drain, demonstrating the utility of molecular markers in evaluating environmental impacts on fish genomes.

The Nile tilapia (*Oreochromis niloticus*) serves as an important model organism in toxicology studies due to its economic significance in aquaculture and its sensitivity to environmental stressors (Khamiss & Hashem, 2012; Hashem *et al.*, 2019; Hashem *et al.*, 2020b; Hashem, 2022). The following study aimed to evaluate the potential protective effects of CS NPs against Mn-induced genotoxicity in the Nile tilapia, a globally significant aquaculture species. We hypothesize that dietary supplementation with CS NPs will mitigate Mn-induced genetic damage in the Nile tilapia.

## MATERIALS AND METHODS

The CS NPs were purchased from Nano Gate (Cairo, Egypt) and used as received for all characterization and experimental procedures. Manganese sulfate ( $\text{MnSO}_4$ ) was obtained from Sigma-Aldrich (St. Louis, MO, USA).

The crystallinity and structural characteristics of the CS NPs were determined using X-ray diffraction (XRD) analysis with a Philips PW 2103 diffractometer (Netherlands) equipped with  $\text{CuK}\alpha$  radiation ( $\lambda = 1.5406 \text{ \AA}$ ). Diffraction data were collected over two angular spans ranging from  $4$  to  $80^\circ$ , at a scanning rate of  $5^\circ/\text{min}$ .

Fourier-transform infrared spectroscopy (FTIR) was performed using a Nicolet iS50 spectrometer (Thermo-Scientific, Bruker Analytical, Germany) equipped with an attenuated total reflectance (ATR) accessory. FTIR/ATR spectra were recorded at room temperature in the range of  $400\text{--}4000\text{cm}^{-1}$  with a resolution of  $4\text{cm}^{-1}$ , providing detailed information on the functional groups present in the CS NPs.

Morphological characteristics and particle size of the CS NPs were investigated using transmission electron microscopy (TEM) (JEOL Model JEM-2100, Tokyo, Japan) at an accelerating voltage of  $200\text{kV}$ . For sample preparation, a drop of the nanoparticle suspension was placed onto a Formvar carbon-coated 300-mesh copper grid (Ted Pella, USA) and allowed to air-dry. Particle size distribution and mean size were analyzed using ImageJ software (National Institutes of Health, USA).

Dynamic light scattering (DLS) was also used to confirm particle size and assess uniformity, while the zeta potential of the CS NPs was measured with a Zetasizer Nano ZS (Malvern Instruments, UK) after the samples were stabilized overnight at room temperature and sonicated.

## 2. Experimental design

All experimental procedures were approved by the Research Ethics Committee of the Genetic Engineering and Biotechnology Research Institute (GEBRI), University of Sadat City (Approval Code: SREC190525B20062), and conducted in accordance with institutional ethical guidelines.

A total of 160 healthy, parasite-free male *Oreochromis niloticus* fingerlings (average weight:  $25 \pm 5$ g; average length:  $10.29 \pm 0.66$ cm) were obtained from local hatcheries licensed by the Ministry of Fisheries. Fish were acclimated for two weeks in 160L glass aquaria containing dechlorinated water, under controlled laboratory conditions: pH 7.6, total hardness 240mg/ L, dissolved oxygen maintained via continuous aeration, ammonia  $< 0.1$  mg/L, nitrite  $< 0.05$ mg/ L, and temperature maintained at  $26 \pm 1^{\circ}\text{C}$  with a 12h light/ 12h dark cycle. Fish were fed a commercial pellet feed (Aller Aqua Egypt) containing 30% protein and 5% fat, at a daily rate of 3% of their body weight.

The 160 fish were randomly distributed into eight groups ( $n = 20$  per group), each housed in separate 160L aquaria. The experimental design included:

- Two Mn concentrations (45 and 27mg/ L),
- Two CS NP supplementation levels (1.0 and 0.5g/ kg of feed) for each Mn concentration,
- A Mn-only group for each concentration (no CS NPs),
- One group treated with 0.5 g/kg CS NPs alone,
- One untreated control group exposed only to dechlorinated water.

Water quality was maintained by replacing 40% of the water every two days to prevent waste accumulation and ensure stable Mn concentrations. The exposure period lasted for 40 days. At the end of the experiment, fish were euthanized using crushed ice, and muscle tissue samples were collected for downstream analyses.

## 3. DNA sampling and SCoT marker analysis

Genomic DNA was extracted from muscle tissue samples of five fish per group using the G-Spin Genomic DNA Extraction Kit (iNtRON Biotechnology, Inc., Korea), following the manufacturer's instructions. DNA quality and concentration were evaluated using a NanoDrop 2000 spectrophotometer (Thermo Fisher Scientific, USA). Extracted DNA samples were stored at  $-20^{\circ}\text{C}$  until further analysis.

Start codon targeted (SCoT) PCR was performed using 10 specific primers (listed in Table 1). This approach was used to assess potential Mn-induced genotoxicity and the protective role of CS NPs.

**Table 1.** SCoT primers and their sequences

| S | PRIMER<br>NAME | SEQUENCE           | S  | PRIMER<br>NAME | SEQUENCE            |
|---|----------------|--------------------|----|----------------|---------------------|
| 1 | SCoT01-14      | CAACAATGGCTACCACCA | 6  | SCoT28-14      | CCATGGCTACCACGCCA   |
| 2 | SCoT02-14      | CAACAATGGCTACCACCC | 7  | SCoT32-14      | CCATGGCTACCACCGCCCT |
| 3 | SCoT16-14      | ACCATGGCTACCACGAC  | 8  | SCoT34-14      | ACCATGGCTACCACCGCGA |
| 4 | SCoT18-14      | ACCATGGCTACCACCGCC | 9  | SCoT35-14      | CATGGCTACCACCGCCCC  |
| 5 | SCoT22-14      | AACCATGGCTACCACCAC | 10 | SCoT36-14      | GCAACAATGGCTACCACC  |

PCR amplification was performed using the Applied Biosystems® ProFlex™ PCR System. Reaction conditions were optimized for all primers, and each reaction was carried out in a total volume of 20µL. The PCR mixture contained 100ng of template DNA (pooled from five fish per treatment group), 10.0µL of 2× Master Mix, 0.4µM of each primer, and deionized water to make up the final volume.

Thermal cycling conditions were as follows:

- Initial denaturation at 94°C for 5 minutes
- 35 cycles of:
  - Denaturation at 94°C for 45 seconds
  - Annealing at 50–58°C for 1 minute (temperature optimized per primer)
  - Extension at 72°C for 1 minute
- Final extension at 72°C for 10 minutes

PCR products were separated via agarose gel electrophoresis and visualized under ultraviolet (UV) light.

#### 4. Band scoring and genetic similarity assessment

The banding patterns generated by each primer were analyzed using ImageJ software. For each sample, bands were scored based on their presence (1) or absence (0), and their relative sizes were documented. These binary data were then used to calculate Jaccard's similarity coefficient as described by **Sneath and Sokal (1973)**, which quantifies genetic similarity between samples based on shared and unique DNA fragments.

To assess genetic relationships among the experimental groups, UPGMA (Unweighted Pair Group Method with Arithmetic Mean) clustering was conducted using GeneTools software. This method generated a dendrogram, a hierarchical tree diagram that visually represents the degree of genetic similarity among the treatment groups based on SCoT marker profiles.

## RESULTS

### 1. Characterization of CS NPs

#### 1.1. X-ray diffraction (XRD) analysis

The XRD pattern of the CS NPs is presented in Fig. (1). The diffractogram exhibits a dominant, extremely broad halo with only very weak and poorly defined reflections observed at approximately  $2\theta$  values of  $26.5^\circ$ ,  $28.1^\circ$ , and  $47^\circ$ . This pronounced peak broadening indicates a near-complete loss of long-range crystalline order, confirming the predominantly amorphous nature of the chitosan nanoparticles. The presence of such a broad halo is characteristic of nanomaterials and supports the nanoscale structure of the CS NPs used in this study. The observed broadening also reflects a substantial reduction in crystalline domain size, which is consistent with nanoparticle formation via methods such as ionotropic gelation. The weak reflections at the specified  $2\theta$  values likely correspond to residual traces of crystalline regions embedded within the largely amorphous nanoparticle matrix.

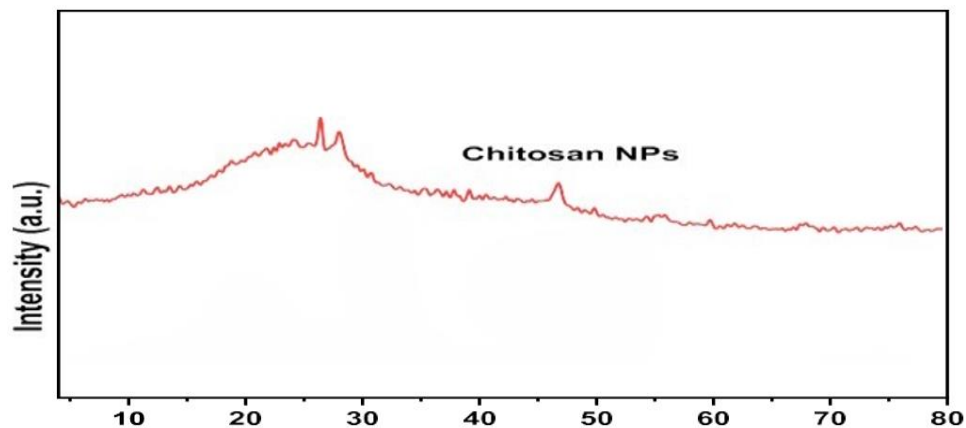


**Fig. 1.** XRD patterns at  $2\theta$  values of chitosan nanoparticles (CS NPs)

#### 1.2. Fourier transform infrared spectroscopy (FTIR) analysis

The attenuated total reflectance Fourier transform infrared (ATR/FTIR) spectra of CS NPs are presented in Fig. (2). The FTIR spectrum of CS NPs revealed specific characteristic bands: a broad band at  $3424\text{cm}^{-1}$  and further characteristic peaks were observed at  $2925\text{cm}^{-1}$ . A group of close peaks at  $1648$ ,  $1549$ ,  $1382$ ,  $1321$ ,  $1155\text{cm}^{-1}$ , and a strong peak at  $1074\text{cm}^{-1}$ . Overall, the FTIR spectra confirms the presence of characteristic functional groups in the CS NPs, indicating retention of the biopolymer's structural features in the obtained CSNP nanoparticles.



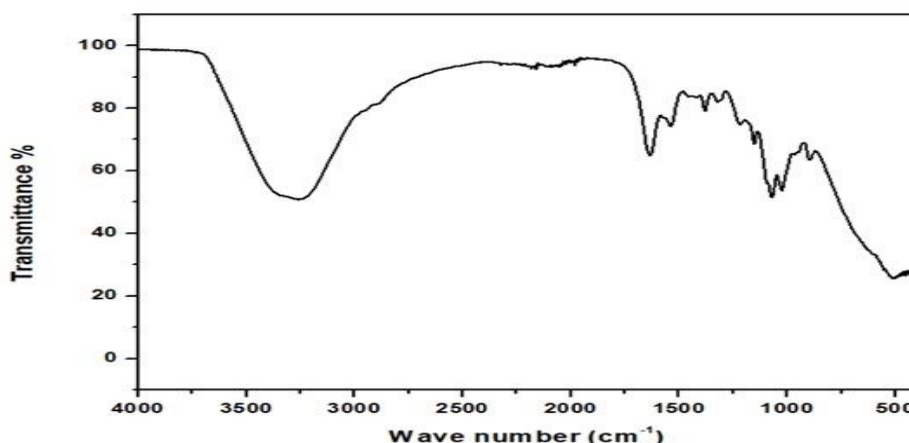


**Fig. 2.** FTIR spectra of chitosan nanoparticles (CS NPs)

### ***1.3. Transmission electron microscopy (TEM) analysis***

A TEM image of CS NPs is displayed in Fig. (3). TEM images revealed that CS NPs were predominantly spheroidal in shape and generally well-dispersed, although some degree of aggregation or clustering was also observed. The average core size of the CS NPs was determined to be  $25 \pm 5$  nm, as confirmed by image analysis using ImageJ software.

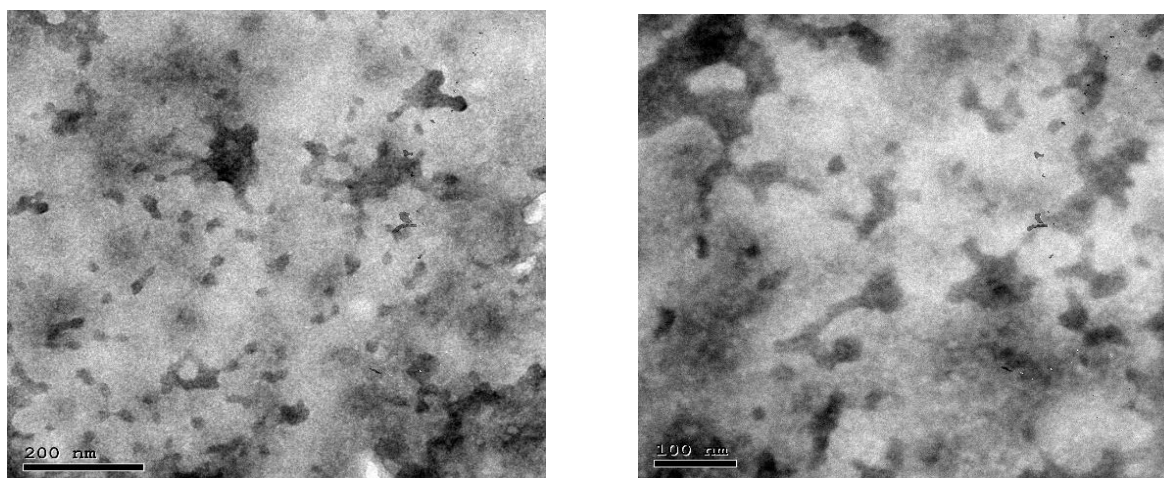


**Fig. 3.** TEM image of chitosan nanoparticles (CS NPs)

### ***1.4. Dynamic light scattering (DLS) analysis***

The size distribution of CS NPs, as determined by DLS, is presented in Fig. (4). DLS analysis revealed a mean hydrodynamic diameter (>80%) of 43.6 nm for the CS NPs, confirming a relatively uniform and unimodal size distribution. The larger hydrodynamic diameter measured by DLS compared to the core size observed in TEM is a common phenomenon and is attributed to the hydration layer surrounding the nanoparticles in aqueous suspension, which is measured by DLS but not visualized in the dry state under TEM.

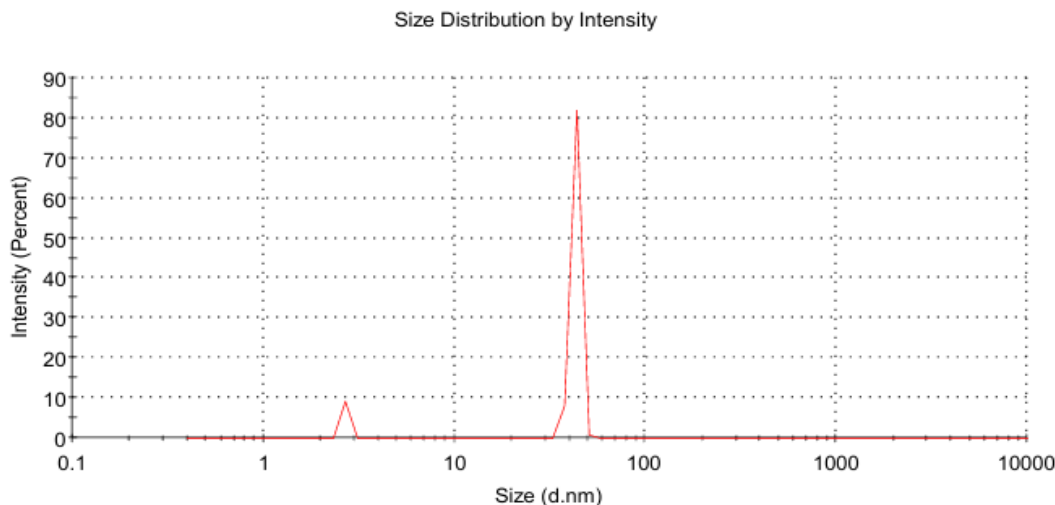
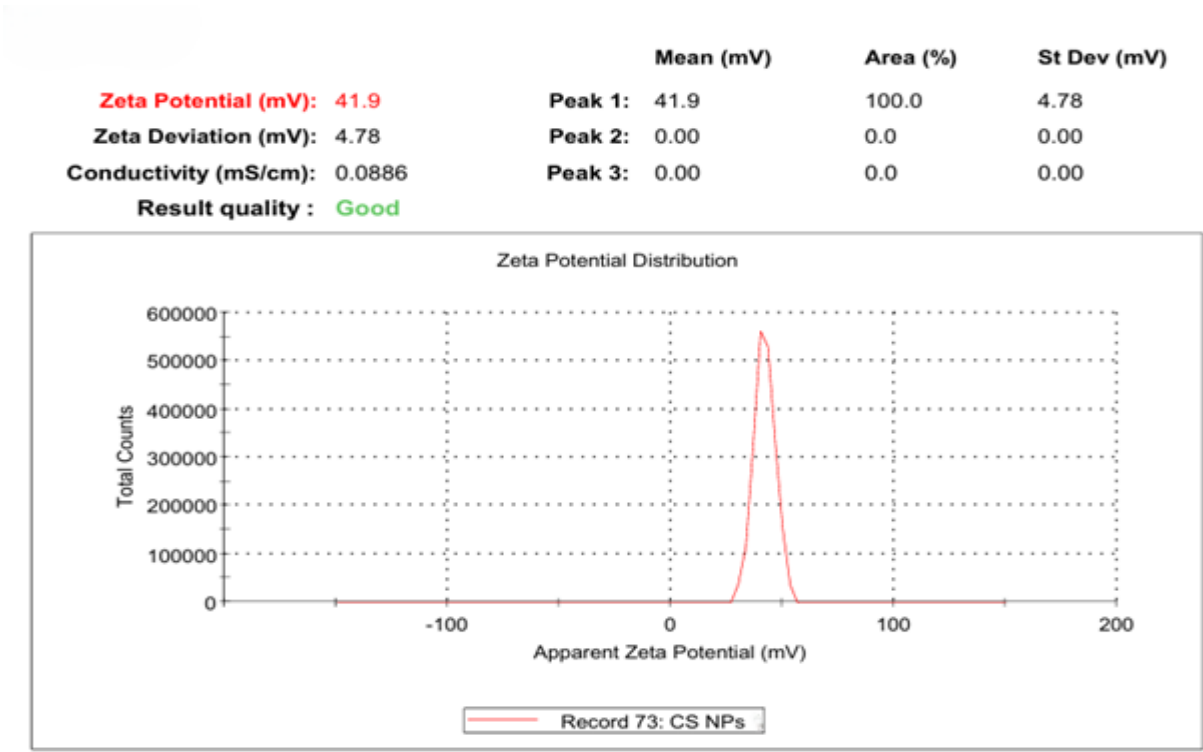


**Fig. 4.** Size distribution of chitosan nanoparticles (CS NPs) as determined by dynamic light scattering (DLS)

### 1.5. Zeta potential analysis

The zeta potential distribution of CS NPs is shown in Fig. (5). The zeta potential of the CS NPs was measured to be +41.9mV using a Zetasizer Nano ZS (Malvern Instruments, UK). The zeta potential distribution graph revealed a single, sharp, and symmetrical peak centered at 41.9mV, indicating a highly homogeneous and unimodal zeta potential distribution within the CSNP sample. The result peak 1 accounts for 100% of the area in the zeta potential distribution, with an acceptable standard deviation of  $\pm 4.78$ mV, further confirming the homogeneity and uniformity of the CSNP surface charge. The Zetasizer Nano ZS software assessed the “Result quality” as “Good,” indicating a reliable and high-quality zeta potential measurement

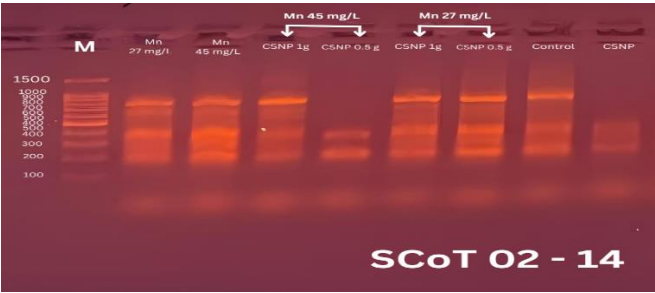
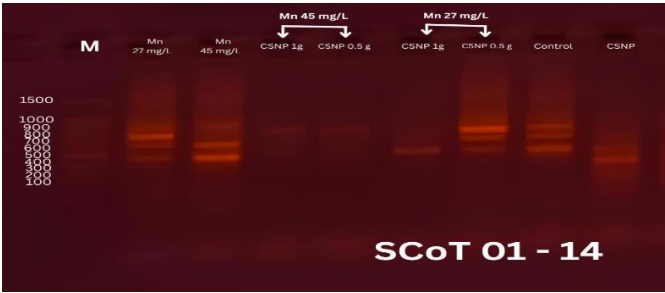




**Fig. 5.** Zeta potential distribution of chitosan nanoparticles (CS NPs)

**2. SCoT molecular markers and genotoxic effect of manganese**

Genomic DNA samples extracted from the muscle tissues of the different groups of *Oreochromis niloticus* exposed to varying manganese (Mn) and chitosan nanoparticles (CS NPs) concentrations, along with controls, were subjected to PCR amplification using ten SCoT primers (SCoT01-14, SCoT02-14, SCoT16-14, SCoT18-14, SCoT22-14, SCoT28-14, SCoT32-14, SCoT34-14, SCoT35-14, and SCoT36-14). The results of these primers are shown in Fig. (6), which illustrates the presence or absence of DNA bands across the different groups. These variations indicate DNA polymorphism and reflect the potential genotoxicity of manganese exposure and CS NPs treatments.



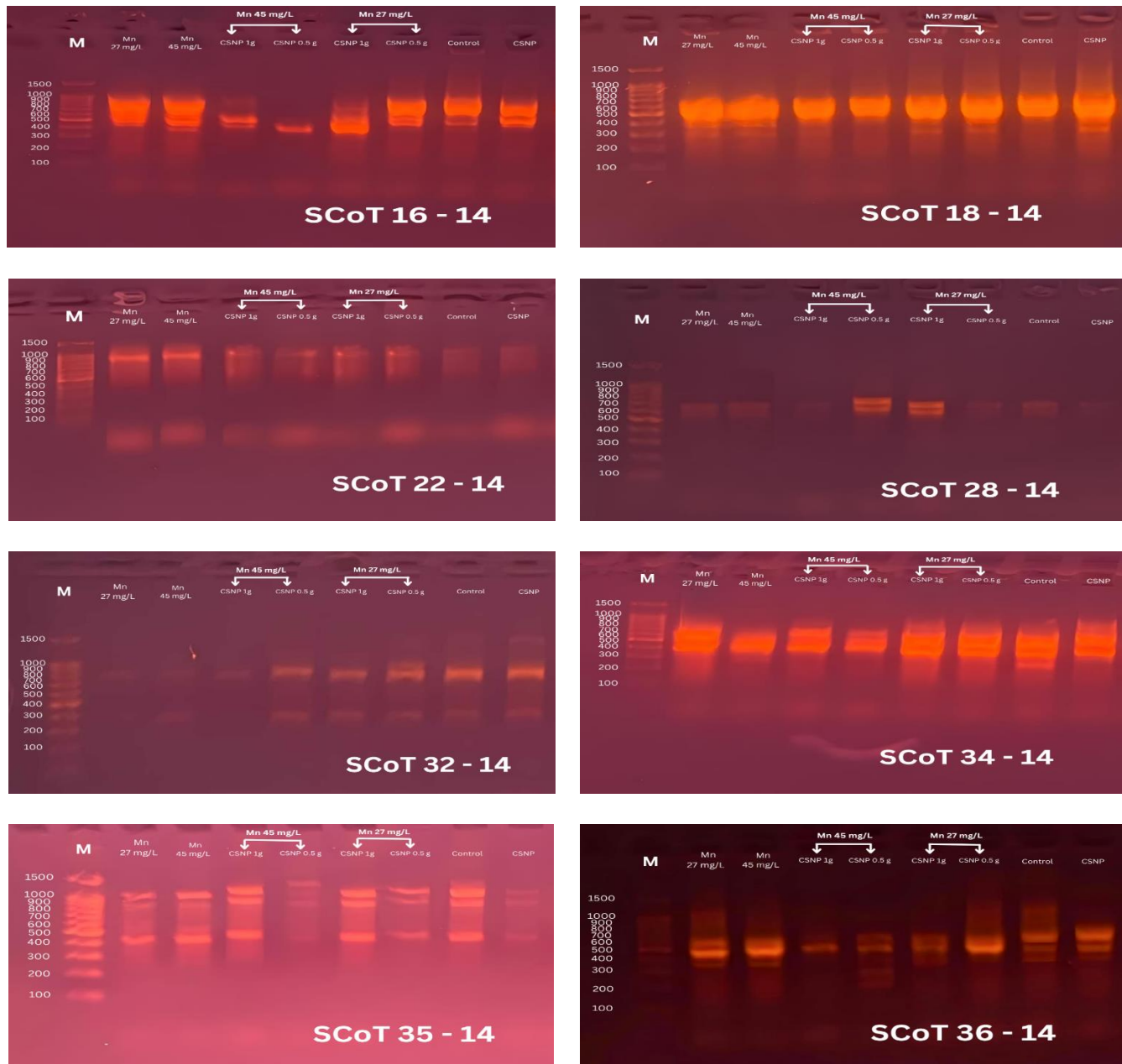


**Fig. 6.** Representative agarose gel electrophoresis image illustrating SCoT banding patterns generated using ten different primers in *Oreochromis niloticus* exposed to different concentrations of manganese and CS NPs. M: DNA marker; CS NPs: chitosan nanoparticles

The detailed results for each primer are presented in Table (2), which was generated based on the banding patterns observed in Fig. (6).

**Table 2.** Polymorphism analysis of SCoT markers across 10 primers

| PRIMER NAME | TOTAL BANDS | UNIQUE BANDS | POLYMORPHIC BANDS | MONOMORPHIC BANDS | POLYMORPHISM (%) |
|-------------|-------------|--------------|-------------------|-------------------|------------------|
| PRIMER 1    | 5           | 0            | 5                 | 0                 | 100.00           |
| PRIMER 2    | 9           | 2            | 7                 | 0                 | 77.78            |
| PRIMER 3    | 7           | 3            | 4                 | 0                 | 57.14            |
| PRIMER 4    | 6           | 1            | 4                 | 1                 | 66.67            |
| PRIMER 5    | 4           | 2            | 2                 | 0                 | 50.00            |
| PRIMER 6    | 6           | 3            | 3                 | 0                 | 50.00            |
| PRIMER 7    | 3           | 1            | 1                 | 1                 | 33.33            |
| PRIMER 8    | 6           | 3            | 3                 | 0                 | 50.00            |
| PRIMER 9    | 10          | 3            | 7                 | 0                 | 70.00            |
| PRIMER 10   | 14          | 9            | 5                 | 0                 | 35.71            |
| TOTAL       | 70          | 27           | 41                | 2                 | 58.57            |

Primer 1 exhibited the highest polymorphism percentage (100%), with all five detected bands being polymorphic and no monomorphic or unique bands observed. In contrast, Primer 7 displayed the lowest polymorphism percentage (33.33%), producing three bands—one unique, one polymorphic, and one monomorphic. Primer 10 generated the highest total number of bands (14), including nine unique bands (64.29% of its bands), with an overall polymorphism percentage of 35.71%.

Band presence/absence analysis revealed that the Mn 27mg/ L + CS NPs 0.5g/ kg group exhibited fewer unique bands compared to the Mn 27mg/ L group across multiple primers. For instance, Primer 10 produced only one unique band in the Mn 27mg/ L + CS NPs group, compared to three in the Mn-only group. Interestingly, treatment with CS NPs alone (0.5g/ kg of feed) appeared to induce a notable genotoxic effect, as reflected by altered banding patterns when compared to the control group. This was particularly evident with primers SCoT01, SCoT02, SCoT18, and SCoT34, which showed group-specific genetic variations and the presence of polymorphic bands.

However, the combination of CS NPs (0.5 g/kg) with Mn (27mg/ L) mitigated these genotoxic effects, as evidenced by reduced genetic alterations and fewer unique bands, indicating a potential protective effect of CS NPs at this concentration.

The dendrogram in Fig. (7) demonstrated distinct clustering patterns among the treatment groups, corroborating the polymorphism data presented in Table (2). Notably, the control group clustered closely with the Mn 27mg/ L + CS NPs 0.5g/ kg group, suggesting a high degree of genetic similarity and underscoring the protective role of CS NPs in reducing Mn-induced genotoxicity. In contrast, groups treated with higher Mn concentrations or higher CS NP dosages (e.g., Mn 45mg/ L, Mn 45mg/ L + CS NPs 0.5 or 1.0g/ kg, and Mn 27mg/ L + CS NPs 1.0g/ kg) showed greater genetic divergence from the control. Additionally, the group treated with CS NPs alone (0.5g/ kg) formed a separate cluster, further indicating nanoparticle-specific genetic impacts.

The branching patterns of the dendrogram provide valuable insights into the genetic relationships among treatment groups, highlighting the effectiveness of CS NPs at 0.5g/ kg in alleviating the genotoxic effects induced by manganese exposure.

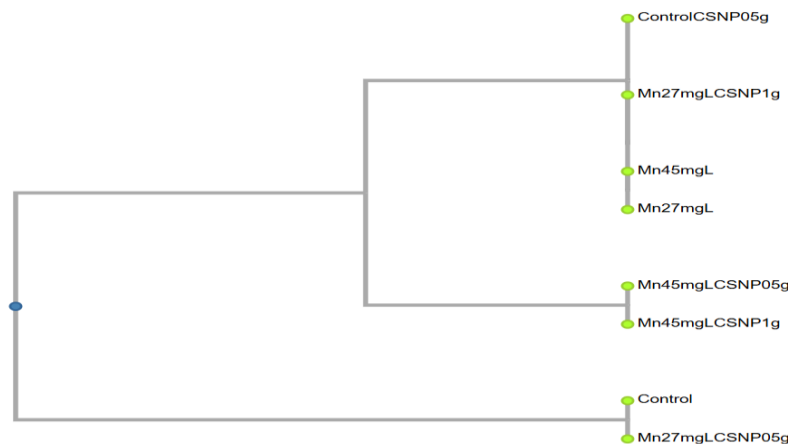


**Fig. 7.** Dendrogram showing the genetic relationships among treatment groups based on SCoT markers analysis

## DISCUSSION

This study aimed to evaluate the protective effects of chitosan nanoparticles (CS NPs) against manganese (Mn)-induced genotoxicity in the Nile tilapia (*Oreochromis niloticus*) using start codon targeted (SCoT) markers. Characterization of the CS NPs through XRD, FTIR, TEM, zeta potential, and DLS provided detailed insights into their physicochemical properties. XRD analysis revealed a predominantly amorphous structure with nanoscale features, consistent with previous studies (Zhang *et al.*, 2012). FTIR spectra confirmed the presence of characteristic functional groups, suggesting that the structural integrity of the biopolymer was retained (Sarbon *et al.*, 2015). TEM images showed that the CS NPs were mostly spheroidal, well-dispersed, and had an average core size of  $25 \pm 5$  nm. Zeta potential analysis revealed a high positive surface charge, attributed to the protonation of amine groups, with values above +30 mV—indicative of good colloidal stability (Zhao *et al.*, 2018). DLS further confirmed the nanoscale range, revealing a hydrodynamic diameter of 43.6 nm, slightly larger than the TEM-derived size due to hydration effects (Alishahi *et al.*, 2011).

FTIR analysis identified several key functional groups. These included a broad band at  $3424\text{cm}^{-1}$  corresponding to overlapping O–H and N–H stretches, suggesting extensive hydrogen bonding; a peak at  $2925\text{cm}^{-1}$  for  $\text{CH}_2$  stretching; and prominent amide bands at  $1648$  and  $1549\text{cm}^{-1}$  corresponding to Amide I (C=O) and Amide II (N–H bending), respectively. Additional peaks were noted at  $1382$ ,  $1321$ ,  $1155$ , and  $1074\text{cm}^{-1}$ , associated with various vibrations of the polysaccharide backbone, confirming the structural integrity of chitosan in nanoparticle form (Sarbon *et al.*, 2015).

The SCoT marker analysis revealed clear distinctions among the treatment groups. The close clustering of the Mn 27 mg/L + CS NPs 0.5 g/kg group with the control group in the dendrogram (Fig. 7) strongly suggests a protective role of CS NPs at this concentration against Mn-induced genotoxicity. This effect is likely due to multiple mechanisms: (i) adsorption and chelation of Mn ions, reducing their bioavailability and DNA interaction (Guibal, 2004; Wan Ngah & Fatinathan, 2010); (ii) enhancement of

DNA repair processes or maintenance of genomic integrity (**Abdel-Wahhab *et al.*, 2016**); and possibly (iii) reduction of oxidative stress, a major pathway of Mn-induced DNA damage (**Obaiah *et al.*, 2020**).

In contrast, groups treated with higher Mn concentrations (45mg/ L) or higher CS NP doses (1.0g/ kg) showed greater genetic divergence from the control, as reflected in both the dendrogram and banding patterns. These groups exhibited a higher number of unique bands, suggesting increased genetic alterations, possibly due to overwhelming oxidative stress or nanoparticle overload. This aligns with reports of dose-dependent nanoparticle toxicity, where excessive CS NP exposure led to oxidative damage and developmental abnormalities in the zebrafish (*Danio rerio*), despite protective effects at lower concentrations.

The observed biphasic (dose-dependent) response highlights the importance of optimizing CS NP dosages in aquaculture settings. At 0.5g/ kg, CS NPs provided significant Geno protection; however, higher doses may activate stress pathways, reversing their beneficial effects.

These results are supported by broader research on chitosan Geno protective properties in aquatic organisms. For instance, **Hussein *et al.* (2021)** and **Abdel-Tawwab *et al.* (2024)** reported that CS NPs reduced DNA damage in the African catfish exposed to Bisphenol-A. Similarly, **Wang and Li (2011)** demonstrated improved growth and survival in *O. niloticus* supplemented with CS NPs, potentially reflecting enhanced cellular and genomic stability. **Heiba *et al.* (2021)** further emphasized the susceptibility of fish genomes to environmental stressors, supporting the use of CS NPs as a mitigative strategy.

Comparative studies in other species also reinforce the dose-specific genomic effects of CS NPs. In plants, **Bhattacharyya *et al.* (2013)** used SCoT markers to confirm genetic fidelity in nanoparticle-treated regenerants. While **Xiong *et al.* (2011)** demonstrated nanoparticle-induced gene expression modulation in peanuts under stress. In mammals, **Abdel-Wahhab *et al.* (2016)** reported that CS NPs reduced oxidative DNA damage in rats, suggesting cross-species applicability of their Geno protective role.

Despite these promising results, several limitations should be considered. This study focused solely on the Nile tilapia, and species-specific genomic responses to Mn and CS NPs may vary (**Barton, 2002**). Additionally, the controlled laboratory environment may not fully replicate field conditions, where multiple stressors interact. Furthermore, while SCoT markers are valuable for detecting DNA polymorphisms (**Collard & Mackill, 2009**), integrating other techniques such as ISSR markers (**Hashem *et al.*, 2020a**) or comet assays could provide a more comprehensive genotoxicity profile.

Future studies should explore the molecular mechanisms underpinning CS NPs' protective effects—particularly gene expression pathways related to oxidative stress, DNA repair, and metal detoxification—using methods like qPCR (**Ahmed *et al.*, 2024**). Research should also address long-term exposure, bioaccumulation, and species variability under both laboratory and natural conditions to ensure safe and effective application in aquaculture.

## CONCLUSION

In this study, CS NPs were predominantly spheroidal in shape, generally well-dispersed, with an average core size of  $25 \pm 5$  nm, and exhibited a high positive surface charge, indicating good colloidal stability. The SCoT markers analysis demonstrated distinct effects among the experimental groups. The clustering of the control group and the Mn 27mg/ L + CS NPs 0.5g/ kg group in the dendrogram suggests that CS NPs at 0.5g/ kg effectively mitigated Mn-induced genotoxic effects at 27mg/ L, indicating a protective role against Mn genotoxicity. In contrast, higher concentrations of Mn and/or CS NPs treatments at 1g/ kg induced more substantial genetic changes in *Oreochromis niloticus*. Additionally, treatment with nanoparticles alone (0.5g/ kg of feed) induced a notable genotoxic effect, as evidenced by the presence or absence of bands compared with the control. Overall, the results highlight that CS NPs at 0.5g/ kg can be a promising tool for protecting *Oreochromis niloticus* from Mn-induced genotoxicity. However, further research is needed to elucidate the underlying molecular mechanisms of CS NPs' protective effects, such as their role in reducing oxidative stress or enhancing DNA repair, and to determine the optimal concentrations for protection against Mn-induced genotoxicity.

## REFERENCES

- Abd El-Naby, F.S.; Naiel, M.A.; Al-Sagheer, A.A. and Negm, S.S.** (2019). Dietary chitosan nanoparticles enhance the growth, production performance, and immunity in *Oreochromis niloticus*. *Aquaculture*, 501: 82-89.
- Abdel-Tawwab, M.; Khalil, R.H.; Younis, N.A.; Abo Selema, T.A.M.; Saad, A.H.; El-Werwary, S.O.M.; Gouda, A.H.; Soliman, A.M.; Shady, S.H.H. and Monier, M.N.** (2024). *Saccharomyces cerevisiae* supplemented diets mitigate the effects of waterborne cadmium toxicity on gilthead seabream (*Sparus aurata* L.): growth performance, haemato-biochemical, stress biomarkers, and histopathological investigations. *Veterinary Research Communications*, 48(1): 69-84.
- Abdel-Wahhab, M.A.; Aljawish, A.; Kenawy, A.M.; El-Nekeety, A.A.; Hamed, H.S. and AbdelAziem, S.H.** (2016). Grafting of gallic acid onto chitosan nanoparticles enhances antioxidant activities in vitro and protects against ochratoxin A toxicity in catfish (*Clarias gariepinus*). *Environ. Toxicol. Pharmacol.*, 41: 279-288.
- Abu-Almaaty, A.H.; Abd-Alaty, H.E.; Abbas, O.A. and Hassan, M.K.** (2020). Genetic relationship between two species of genus *Dicentrarchus* based on SCoT markers and SDS-PAGE. *Egyptian Journal of Aquatic Biology & Fisheries*, 24(5): 393-402.
- Ahmed, S.A.A.; Ibrahim, R.E.; Younis, E.M.; Abdelwarith, A.A.; Faroh, K.Y.; El Gamal, S.A.; Badr, S.; Khamis, T.; Mansour, A.T.; Davies, S.J. and ElHady, M.** (2024). Antagonistic Effect of Zinc Oxide Nanoparticles Dietary Supplementation Against Chronic Copper Waterborne Exposure on Growth, Behavioral, Biochemical, and Gene Expression Alterations of African



- Catfish, *Clarias gariepinus* (Burchell, 1822). Biological Trace Element Research, 202(12): 5697-5713.
- Alishahi, A.; Mirvaghefi, A.; Tehrani, M.R.; Farahmand, H.; Koshio, S.; Dorkoosh, F.A. and Elsabee, M.Z.** (2011). Chitosan nanoparticle to carry vitamin C through the gastrointestinal tract and induce the non-specific immunity system of rainbow trout (*Oncorhynchus mykiss*). Carbohydr. Polym., 86(1): 142-146.
- Amirmoradi, B.; Talebi, R. and Karami, E.** (2012). Comparison of genetic variation and differentiation among annual *Cicer* species using start codon targeted (SCoT) polymorphism, DAMD-PCR, and ISSR markers. Plant Syst. Evol., 298(9): 1679-1688.
- Authman, M.M.; Abbas, H.H. and Abbas, W.T.** (2013). Assessment of metal status in drainage canal water and their bioaccumulation in *Oreochromis niloticus* fish in relation to human health. Environmental Monitoring and Assessment, 185: 891-907.
- Barton, B.A.** (2002). Stress in fishes: a diversity of responses with particular reference to changes in circulating corticosteroids. Integr Comp Biol, 42: 517-525.
- Bayomy, M.F.F.; Alne-na-ei, A.A.; Gaber, H.S.; Sayed, H.A. and Khairy, D.M.** (2015). Environmental and physiological impacts of heavy metals on Nile tilapia (*Oreochromis niloticus*). Journal of Bioscience and Applied Research, 1(2): 52-58.
- Bhattacharyya, P.; Kumaria, S.; Kumar, S. and Tardon, P.** (2013). Start Codon Targeted (SCoT) marker reveals genetic diversity of *Dendrobium nobile* Lindl., an endangered medicinal orchid species. Gene, 529(1): 21-26.
- Boyd, C.E.; D'abramo, L.R.; Glencross, B.D.; Huyben, D.C.; Juarez, L.M.; Lockwood, G.S.; Mcnevin, A.A.; Tacon, A.G.; Teletchea, F. and Tomasso Jr., J.R.** (2020). Achieving sustainable aquaculture: historical and current perspectives and future needs and challenges. J. World Aquacult. Soc., 51: 578-633.
- Bukola, D.; Zaid, A.; Olalekan, E. and Falilu, A.** (2015). Consequences of anthropogenic activities on fish and the aquatic environment. Poultry, Fisheries & Wildlife Sciences, 3(2): 1-12.
- Cabo, S.; Ferreira, L.; Carvalho, A.; Martins-lobes, P.; Martin, A. and Lima-Brito, J.E.** (2014). Potential of Start Codon Targeted (SCoT) markers for DNA fingerprinting of newly synthesized tritordeums and their respective parents. J. Appl. Genet., 55(3): 307-312.
- Carvalho, G.R. and Hauser, L.** (1998). Advances in the molecular analysis of fish population structure. Ital. J. Zool., 65: 21-33.
- Collard, B.C.Y. and Mackill, D.J.** (2009). Start Codon Targeted (SCoT) Polymorphism: a simple novel DNA marker technique for generating gene-targeted markers in plants. Plant Mol. Biol. Rep., 27: 86-93.
- El-Naggar, M.M.; Salaah, S.; Suloma, A.; Khalil, M.T. and Emam, W.W.** (2022). Impact of chitosan and chitosan nanoparticles on reducing heavy metals in the Nile tilapia, *Oreochromis niloticus*. Egypt J Aquat Biol Fish, 26(2): 859-874.
- El-Shafei, H.A.; Asaad, G.F.; Elkhateeb, Y.A.; El-Dakrouy, W.A.; Hamed, H.A.; Hassan, A. and Nomier, Y.A.** (2021). Antimicrobial and hepatoprotective effect of chitosan nanoparticles in-vitro and in-vivo study. J. Pharm. Res. Int., 33: 244-264.

- Fang-Yong, Ch. and Ji-Hong, L.** (2014). Germplasm genetic diversity of *Myrica rubra* in Zhejiang Province studied using interprimer binding site and start codon-targeted polymorphism markers. *Sci. Hortic.*, 170: 169-175.
- Guibal, E.** (2004). Interactions of metal ions with chitosan-based sorbents: a review. *Separation and Purification Technology*, 38(1): 43-74.
- Hashem, M.H.** (2022). Early sexing of *Tilapia nilotica* (*Oreochromis niloticus*) by using short sequence repeats (SSRs) molecular markers. *Damanhour Journal of Veterinary Sciences*, 8: 22-25.
- Hashem, M.H.; Abdel-Azim, R.M.; Abel-Rahman, M.M. and Mousa, I.E.** (2019). Brackish water for cultivation of *Oreochromis niloticus* with sex-reversed female by diethylstilbesterol. *International Multidisciplinary Scientific GeoConference: SGEM*, 19(3.1): 65-72.
- Hashem, M.; Tayel, S.I.; Sabra, E.A.; Yacoub, A.M. and Heiba, A.A.** (2020a). Impact of the water quality of El-Rahawy Drain on some genetic and histopathological aspects of *Oreochromis niloticus*. *Egyptian Journal of Aquatic Biology and Fisheries*, 24(2): 19-38.
- Hashem, M.H.; Meshhal, D.T.; Mohamed, F.A.S. and Khamiss, O.A.** (2020b). Establishment of a cell culture system and characterization of the primary cultures from different organs of the Nile tilapia *Oreochromis niloticus*. *Egyptian Journal of Aquatic Biology and Fisheries*, 24(4): 127-137.
- Heiba, A.A.; Amal, M.Y.; Ebrahim, A.S.; Reham, M.A. and Medhat, H.H.** (2021). Biochemical, histopathological, and genetic impacts of River Nile pollutants on the Nile tilapia (*Oreochromis niloticus*). *Egyptian Journal of Aquatic Biology and Fisheries*, 25(3): 883-899.
- Hussein, N.M.; Ma Saeed, R.; Shaheen, A.S. and Hamed, H.S.** (2021). Ameliorative role of chitosan nanoparticles against bisphenol-A induced behavioral, biochemical changes and nephrotoxicity in the African catfish, *Clarias gariepinus*. *Egypt. J. Aquat. Biol. Fish.* 25, 493-510.
- Khamiss, O. and Hashem, M.H.** (2012). Developing a cell culture system from Nile tilapia (*Oreochromis niloticus*, L.) ovarian tissue in Egypt. *IOSR Journal of Agriculture and Veterinary Science*, 1(3): 8-12.
- Kumar, N.S. and Gurusubramanian, G.** (2011). Random amplified polymorphic DNA (RAPD) markers and its applications. *Sci. Vis.* 11(3): 116-124.
- Lall, S.P.** (2002). The minerals. In: *Fish Nutrition* (Halver, J.E. & Hardy, R.W. eds), 3rd edn., pp. 259-308. Academic Press, San Diego, CA.
- Liu, Z.J. and Cordes, J.F.** (2004). DNA marker technologies and their applications in aquaculture genetics. *Aquaculture*, 238(1-4): 1-37.
- Monier, M.N.; Soliman, A.M. and Al-Halani, A.A.** (2023). The seasonal assessment of heavy metals pollution in water, sediments, and fish of grey mullet, red seabream, and sardine from the Mediterranean coast, Damietta. *North Egypt Reg Stud Mar Sci*, 57:102744.
- Obaiah, J.; Vivek, C.; Padmaja, B.; Sridhar, D. and Peera, K.** (2020). Cadmium toxicity impact on aquatic organisms oxidative stress: implications for human health safety

- and environmental aspects. A review. Intl J Sci Res, 9:2277-8616.
- Poczai, P.; Varga, I.; Laos, M.; Cseh, A.; Bell, N.; Valkonen, H.P. and Hyvonen, J.** (2013). Advances in plant gene-targeted and functional markers: a review. Plant Methods, 9(1):6.
- Que, Y.X.; Pan, Y.B.; Lu, Y.H.; Yang, C.; Yang, Y.T.; Huang, N. and Xu, L.P.** (2014). Genetic analysis of diversity within a Chinese local sugarcane germplasm based on start codon targeted polymorphism. Bio. Med. Res. Int., 468375.
- Sarbon, N.M.; Sandanamsamy, S.; Kamaruzaman, S.F.S. and Ahmad, F.** (2015). Chitosan extracted from mud crab (*Scylla olivacea*) shells: physicochemical and antioxidant properties. J Food Sci Technol, 52:4266-4275.
- Sharma, M.; Thakur, J. and Verma, S.** (2019). Behavioural responses in effect to chemical stress in fish: a review. Intl J Fish Aquatic Stud, 7(1):1-5.
- Shiau, S.Y. and Hsieh, J.F.** (2001). Quantifying the dietary potassium requirement of juvenile hybrid tilapia (*Oreochromis niloticus* × *O. aureus*). Br. J. Nutr. 85, 213-218.
- Sneath, P.H.A. and Sokal, R.R.** (1973). *Numerical taxonomy; the principles and practice of numerical classification*. San Francisco: Freeman Medical Research Council Microbial systematic Unit. Leicester, England and Dept. Ecology and Evolution State Univ. New York, Stony Brook, NY.
- Wan Ngah, W.S.W. and Fatinathan, S.** (2010). Pb (II) biosorption using chitosan and chitosan derivatives beads: Equilibrium, ion exchange and mechanism studies. Journal of Environmental Sciences, 22(3): 338-346.
- Wang, Y. and Li, J.** (2011). Effects of chitosan nanoparticles on survival, growth and meat quality of tilapia. *Oreochromis Nilotica* Nanotoxicology, 5(3):425-431.
- Xiong, F.; Zhong, R.; Han, Z.; Jiang, J.; He, L.; Zhuang, W. and Tang R.** (2011). Start Codon Targeted polymorphism for evaluation of functional genetic variation and relationships in cultivated peanut (*Arachis hypogaea* L.). Genotypes. Mol. Biol. Rep., 38(5): 3487-3494.
- Zhang, W.; Zhang, J.; Jiang, Q. and Xia, W.** (2012). Physicochemical and structural characteristics of chitosan nanopowders prepared by ultrafine milling. Carbohydrate Polymers, 87: 1-6.
- Zhao, D.; Yu, S.; Sun, B.; Gao, S.; Guo, S. and Zhao, K.** (2018). Biomedical applications of chitosan and its derivative nanoparticles. Polymers, 10 (4), 462.